Structures of the Cadmium, Mercury, and Zinc Thiolate Clusters in Metallothionein: XAFS Study of Zn_7-MT, Cd_7-MT, Hg_7-MT, and Hg_{18}-MT Formed from Rabbit Liver Metallothionein 2

D. T. Jiang,[†] Steven M. Heald,[‡,§] T. K. Sham,*[,†] and Martin J. Stillman*[,†]

Contribution from the Department of Chemistry, University of Western Ontario, London, Ontario N6A 5B7, Canada, and Department of Applied Science, Brookhaven National Laboratory, Upton, New York 11973

Received February 9, 1994[⊗]

Abstract: The structural properties of zinc, cadmium, and mercury metallothioneins (MT) have been studied at 77 K using X-ray absorption fine structure spectroscopy (XAFS). The nearest neighbor bond lengths and coordination numbers for Zn_7-MT 2 and Cd_7-MT 2 are in close agreement with the previously reported values. Strikingly different structural parameters have been obtained for the mercury-containing metallothioneins. For Hg_7-MT 2 the nearest neighbor Hg-S bond length and coordination number are determined to be 2.33 ± 0.02 Å and 2, respectively. A new structure is proposed for Hg_7-MT 2 formed by addition of Hg^{2+} to Zn_7-MT at pH 7 in which each Hg(II) is coordinated by four thiolate sulfur but with two unusually short bonds and two unusually long bonds which exhibit a much larger disorder than the shorter bonds. For the Hg_{18}-MT 2 species formed by adding Hg^{2+} to *apo*-MT 2 at pH 2, the local structure is shown to involve nearest neighbor Hg-S bond lengths of 2.42 ± 0.026 Å with 2-fold sulfur coordination plus an Hg-Cl shell at 2.57 ± 0.03 Å with an apparent coordination number 0.61 and large disorder.

Introduction

The structural chemistry of biological metal-sulfur clusters is remarkable in its complexity and variety. Although the iron-sulfur proteins have long been studied, the characterization of the binding site in the cadmium and zinc metallothioneins from NMR[1] and X-ray diffraction[2] studies introduced a new and diverse class of natural cluster compounds that involves clusters of metals with both bridging and terminal thiolate ligands. The metallothioneins are found ubiquitously throughout nature.[3] Mammalian metallothioneins typically have a primary sequence that involves the 20 cysteines in a number of cys-x-cys units along a peptide chain of 61 or 62 amino acids. A wide range of metal ions bind to mammalian metallothioneins.[3,4] A variety of spectroscopic techniques have been used to study the structures of metallothionein[1-11]; particularly, the metal binding reactions and metal binding structures of Cd(II),[1-4] Zn(II),[1-3] Co(II),[6] Cu(I),[7] Ag(I),[9] and Hg(II)[5,10,11] have been most thoroughly studied. The single most consistent feature of metal binding to the mammalian protein has been the discovery of three structural motifs characterized by metal-thiolate stoichiometries of M_7-S_{20} (Cd_7-MT;[1-4] Zn_7-MT;[1-4] Co_7-MT[6]), M_{12}-

* Address correspondence to these authors at the U.W.O. or Internet: Sham@UWO.CA or Stillman@UWO.CA or Fax (519)661-3022.

[†] University of Western Ontario.

[‡] Brookhaven National Laboratory.

[§] Current address: Argonne National Laboratory, Building 360, Argonne, IL 60439.

[⊗] Abstract published in *Advance ACS Abstracts,* October 15, 1994.

(1) (a) Otvos, J. D.; Armitage, I. M. *Proc. Natl. Acad. Sci. U.S.A.* **1980**, *77*, 7094-7098. (b) Boulanger, Y.; Armitage, I. M.; Miklossy, K.-A.; Winge, D. R. *J. Biol. Chem.* **1982**, *257*, 13717-13719. (c) Messerle, B. A.; Schaffer, A.; Vasak, M.; Kagi, J. H. R.; Wuthrich, K. *J. Mol. Biol.* **1992**, *225*, 433-443.

(2) (a) Robbins, A. H.; McRee, D. E.; Williamson, M.; Collett, S. A.; Xuong, N. H.; Furey, W. F.; Wang, B. C.; Stout, C. D. *J. Mol. Biol.* **1991**, *221*, 1269-1293. (b) Robbins, A. H.; Stout, C. D. In *Metallothioneins*; Stillman, M. J., Shaw, C. F., III, Suzuki, K. T., Eds.; VCH: New York, 1992; Chapter 3, pp 31-54.

(3) (a) Kagi, J. H. R.; Nordberg, M., Eds. *Metallothionein I*; Birkhaeuser: Basel, 1979. (b) Kagi, J. H. R.; Kojima, Y. Eds. *Metallothionein II*; Birkhaeuser: Basel, 1987. (c) Stillman, M. J., Shaw, C. F.; III, Suzuki, K. T., Eds. *Metallothioneins*; VCH: New York, 1992. (d) Shaw, C. F.; Stillman, M. J.; Suzuki, K. T. In *Metallothioneins*; Stillman, M. J., Shaw, C. F., III, Suzuki, K. T., Eds.; VCH: New York, 1992; Chapter 1, pp 1-13. (e) Stillman, M. J. In *Metallothioneins*; Stillman, M. J., Shaw, C. F., III, Suzuki, K. T., Eds.; VCH: New York, 1992; Chapter 4, pp 56-120.

(4) (a) Stillman, M. J.; Cai, W.; Zelazowski, A. J. *J. Biol. Chem.* **1987**, *262*, 4358-4548. (b) Stillman, M. J.; Zelazowski, A. J. *J. Biol. Chem.* **1988**, *263*, 6128-6133.

(5) (a) Stillman, M. J.; Law, A. Y. C.; Szymanska, J. A. In *Chemical Toxicology and Clinical Chemistry of Metals*; Brown, S. S., Savory, J., Eds.; Harcourt Brace: London, 1983; pp 271-274. (b) Johnson, B. A.; Armitage, I. M. *Inorg. Chem.* **1987**, *26*, 3139-3145. (c) Vasak, M.; Kagi, J. H. R. In *Metal Ions in Biological Systems*; Sigel, H., Ed.; Marcel Dekker: New York, 1983; p 213. (d) Dean, P. A. W.; Law, A. Y. C.; Szymanska, J. A.; Stillman, M. J. *Inorg. Chim. Acta* **1983**, *78*, 275-279.

(6) Vasak, M.; Kagi, J. H. R. *Proc. Natl. Acad. Sci. U.S.A.* **1981**, *78*, 6709-6713.

(7) (a) Nielson, K. B.; Winge, D. R. *J. Biol. Chem.* **1984**, *259*, 4941-4946. (b) George, G. N.; Byrd, J.; Winge, D. R. *J. Biol. Chem.* **1988**, *263*, 8199-8203. (c) George, G. N.; Winge, D. R.: Stout, C. D.; Cramer, S. P. *J. Inorg. Biochem.* **1986**, *27*, 213-220. (d) Smith, T. A.; Lerch, K.; Hodgson, K. O. *Inorg. Chem.* **1986**, *25*, 4677-4680. (e) Green. A. R.; Presta, A. P.; Gasyna, Z.; Stillman, M. J. *Inorg. Chem.* **1994**, *33*, 4159-4168.

(8) (a) Charnock, J. M.; Garner, C. D.; Abrahams, I. L.; Arber, J. M.; Hasnain, S. S.; Henehan, C.; Vasak, M. *Physica B* **1989**, *158*, 93-94. (b) Abrahams, I. L.; Bremner, I.; Diakun, G. P.; Garner, C. D.; Hasnain, S. S.; Ross, I.; Vasak, M. *Biochem. J.* **1986**, *236*, 585-589. (c) Abrahams, I. L.; Garner, C. D.; Bremner, I.; Diakun, G. P.; Hasnain, S. S. *J. Am. Chem. Soc.* **1985**, *107*, 4596-4597. (d) Garner, C. D.; Hasnain, S. S.; Bremner, I.; Bordas, J. *J. Inorg. Biochem.* **1982**, *16*, 253-256. (e) Wright, J. G.; Tsang, H. T.; Penner-Hahn, J. E.; O'Halloran, T. V. *J. Am. Chem. Soc.* **1990**, *112*, 2434-2435.

(9) (a) Zelazowski, A. J.; Gasyna, Z.; Stillman, M. J. *J. Biol. Chem.* **1989**, *264*, 17091-17099. (b) Zelazowski, A. J.; Stillman, M. J. *Inorg. Chem.* **1992**, *31*, 3363-3370.

(10) (a) Cai, W.; Stillman, M. J. *J. Am. Chem. Soc.* **1988**, *110*, 7872-7873. (b) Lu, W.; Zelazowski, A. J.; Stillman, M. J. *Inorg. Chem.* **1993**, *32*, 919-926.

(11) Lu, W.; Stillman, M. J. *J. Am. Chem. Soc.* **1993**, *115*, 3291-3299.

0002-7863/94/1516-11004$04.50/0 © 1994 American Chemical Society

S_{20} (Cu_{12}-MT;[3,7,8] Ag_{12}-MT[3,9]), and, recently, M_{18}-S_{20} (Hg_{18}-MT;[10] and Ag_{18}-MT[9]). To date all metals binding in vitro to the mammalian protein have exhibited one of these three stoichiometric ratios.[3d] Although Cd(II), Zn(II), and Co(II) exhibit a single structural motif (the M_7-S_{20} structure, which is associated with tetrahedral coordination of the metal by both bridging and terminal cysteinyl thiolates),[1,2,3b] recent spectroscopic studies from our laboratory have shown that Hg(II), Ag(I), and possibly Cu(I) can adopt more than one coordination geometry;[9-11] where the geometry adopted depends on the specific metal−thiolate stoichiometric ratio in the binding site.[3d,4] Significantly, these recent spectroscopic data show that Hg(II) binds to rabbit liver metallothionein with the stoichiometric ratios of Hg_7-S_{20}, Hg_{11}-S_{20}, and Hg_{18}-S_{20}.[10,11] Although these stoichiometries are now well-established, only one structural analysis has previously been reported for Hg-containing metallothionein[12] in which a Hg−S bond length of 2.42 Å and a coordination number of 3 were reported, although previously a coordination number of 4 had been determined for M_7-MT species with M = Zn(II), Cd(II), and Co(II).

X-ray absorption fine structure spectroscopy (XAFS) techniques (X-ray absorption near edge, XANES, and extended X-ray absorption fine structure, EXAFS) have been used extensively to probe the structures of metalloproteins[12] and, in particular, metallothioneins.[7,8,12] EXAFS data for copper metallothioneins have suggested Cu−S bond lengths of 2.20−2.27 Å.[7b-d] EXAFS studies on Zn_7-MT and Cd_7-MT[8a-d] provided excellent values for the M−S bond lengths—values that complemented those obtained by analysis of X-ray diffraction.[2] In this paper we report structural parameters obtained by analysis of metal X-ray absorption fine structure spectra for Zn(II), Cd(II), and Hg(II) containing rabbit liver metallothionein. Values for the Zn−S, Cd−S, and Hg−S bond lengths, the Zn(II), Cd(II), and Hg(II) coordination numbers, and the XAFS Debye−Waller factors of the bonds are reported for the Zn_7-MT, Cd_7-MT, Hg_7-MT, and Hg_{18}-MT species. We interpret the structural data in terms of the previously reported chemical and spectroscopic properties of Hg_n-MT (n = 7 and 18) formed when Hg(II) is added to *apo*-MT, Zn_7-MT, and Cd_7-MT.

Experimental Section

Sample Preparation. Rabbit liver Zn_7-MT was induced and isolated as isoforms 1 and 2 as previously described.[10,11,13] Metal substitution was carried out by adding $CdCl_2$ or $Hg(NO_3)_2$ to solutions of Zn_7-MT.[10,11] Solutions of Zn_7-MT (isoforms 1 and 2) and Cd_7-MT 2 were prepared at pH 7; solutions of Hg_7-MT (isoforms 1 and 2) were prepared from Zn_7-MT 1 and 2 at pH 7. The sample was freeze dried from a solution at pH 7. Hg_{18}-MT 2 was prepared at pH 2 by adding $Hg(NO_3)_2$ to Zn_7-MT 2 (essentially, *apo*-MT 2) held at pH 2 with HCl. The sample was freeze dried from a solution at pH 2. The circular dichroism (CD) spectrum was used to monitor cluster formation for each species.[10,11] The freeze-dried samples were stored at −20 °C before use. Spectroscopic data shown here are for samples prepared from Zn_7-MT 2. XAFS spectra of Hg_7-MT 1 prepared from Zn_7-MT 1 are not shown here, but the features are near identical with those of Hg_7-MT 2.

Data Collection. The XAFS experiments were performed on beam line X11A at the National Synchrotron Light Source (NSLS), Brookhaven National Laboratory, with the storage ring providing a 2.58-GeV electron beam at a current of 140−190 mA. A Si(111) double-crystal monochromator was used with the entrance slit set at 0.5 mm for Zn K-edge and Hg L_3-edge and at 0.25 mm for Cd K-edge. The monochromator was detuned to 80% of the maximum intensity at 30 eV above Hg L_3-edge and Zn K-edge to minimize the harmonic contamination in the incident beam. For measurements at Cd K-edge where the higher order contamination is not a factor, the monochromator was tuned to its maximum intensity.

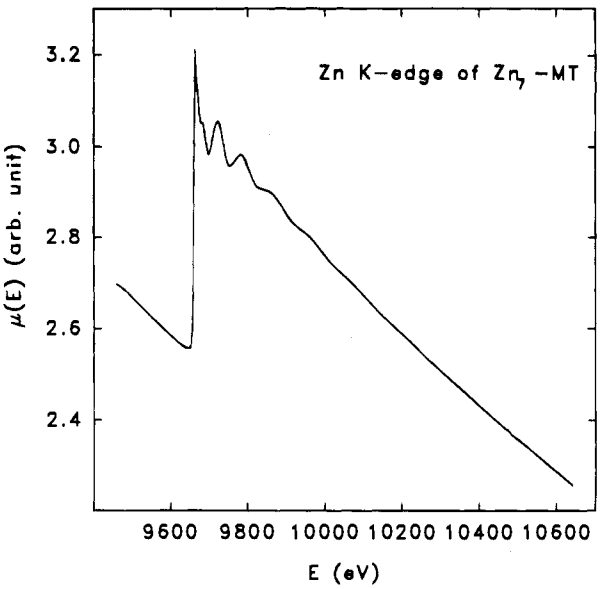

Figure 1. A typical raw data set in this work. Raw data sets were obtained from averaging 5 to 12 scans depending on the signal-to-noise ratio of a particular sample.

The freeze-dried samples were pressed into a rectangular shape (13 × 3.7 mm^2) copper frame using a mechanical punch; care was taken to make the sample thickness as uniform as possible. The two open ends of copper holder were sealed by single-side adhesive Kapton tape (30 μm in thickness) and aluminum foil (7.7 μm in thickness) was placed between the protein sample and the Kapton tape to increase the thermal conductivity to the sample.

The XAFS measurements were carried out at 77 K in transmission mode for all the samples. XAFS of Zn- and Cd-containing metallothioneins were measured at the corresponding K-edges, and Hg-containing metallothioneins were measured at the Hg L_3-edge. A short ionization chamber (6 in. in length) filled with nitrogen gas was used for monitoring the incoming beam intensity. The transmitted beam intensity was detected by a long ionization chamber (12 in. in length) filled with argon and krypton gas for measurements at Zn K-edge/Hg L_3-edge and Cd K-edge, respectively.

The samples were kept frozen all the time, including the transportation to the XAFS experimental site. No changes in either the near edge region or the EXAFS region were observed during data collection, which typically last about 4 h for each sample. Thus X-ray radiation does not seem to cause any significant damage to the proteins under the given conditions.

Results and Data Analysis

Figure 1 shows a typical raw data set for Zn_7-MT before data reduction. The reproducibility of data from multiple scans for each sample was checked in both E (X-ray photon energy) space and k (photoelectron wavenumber) space to identify any suspicious features in the spectra due to experimental artifacts. The data reduction procedure used was as the follows. The EXAFS interference function is defined by $\chi(k) = [\mu(E) - \mu_0(E)]/\mu_0(E)$, where E and k are, respectively, the X-ray photon energy and the wavenumber of the photoelectron excited by the X-ray photon and $\mu_0(E)$ is the atomic absorption coefficient. The experimental energy origin is defined at the inflection point of the absorption threshold, $E_{\text{inflection}}$. The k^3 weighted $\chi(k)$ of the metallothioneins (shown in Figure 2) were extracted from

(12) Hasnain, S. S. *Top. Curr. Chem.* **1988**, *147*, 73−93.
(13) Zelazowski, A. J.; Szymanska, J. A.; Witas, H. *Prep. Biochem.* **1980**, *10*, 495−505.

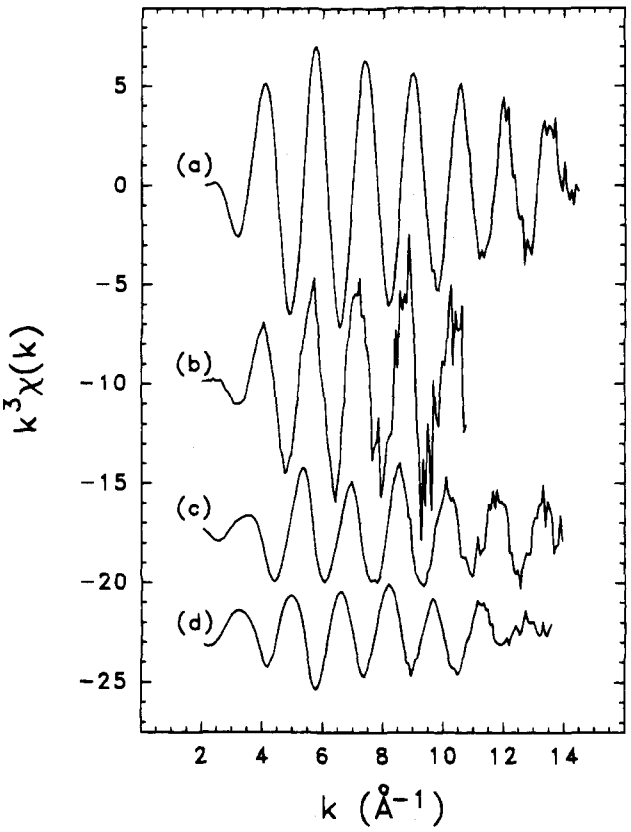

Figure 2. $k^3\chi(k)$ of metallothioneins obtained at 77 K: (a) Zn_7-MT 2; (b) Cd_7-MT 2; (c) Hg_7-MT 2; and (d) Hg_{18}-MT 2. The spectra are vertically displaced for clarity. Notice the factor of ca. 2 difference in the EXAFS amplitude between the data for Zn_7/Cd_7-MT 2 and Hg_7/Hg_{18}-MT 2.

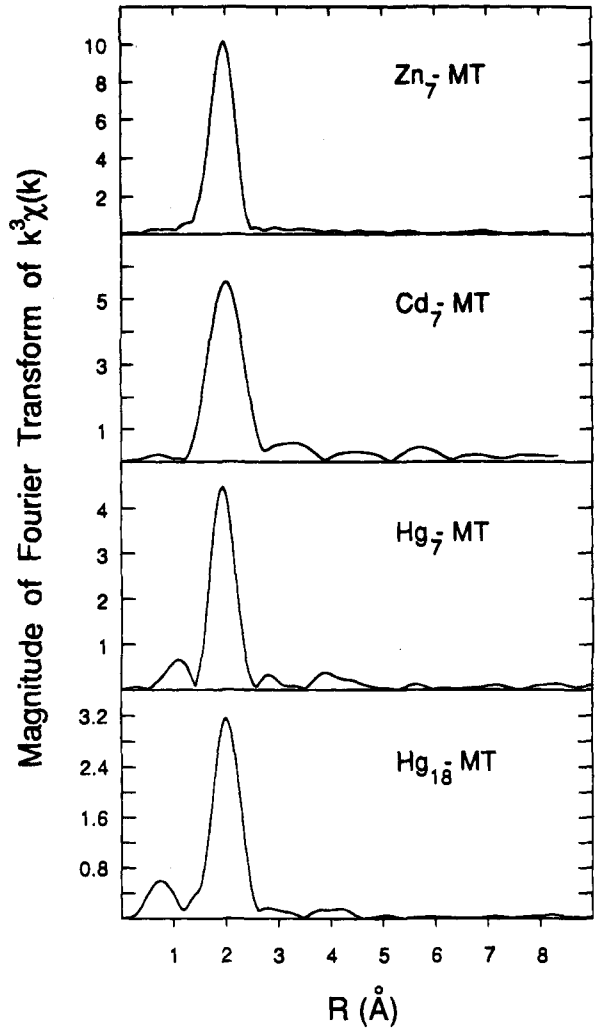

Figure 3. The magnitude of the Fourier transform of $k^3\chi(k)$; the Hamming window was used, and the k-space data ranges used in the transform are as follows: Zn_7-MT 2, 2.10–14.50 Å^{-1}; Cd_7-MT 2, 2.75–10.67 Å^{-1}; Hg_7-MT 2, 2.00–14.02 Å^{-1}; and Hg_{18}-MT 2, 2.64–13.34 Å^{-1}. The positions of the peaks are shifted a few tenths of an angström from the actural interatomic distances because of the EXAFS phase shift.

the raw data following the usual procedure,[14a] in which the pre-edge background was removed by the Victoreen function and the post-edge background was removed by a 3-section cubic spline fit or a 7th order polynomial, and then the data were normalized by the edge jump obtained by extrapolation of a stright line fit above the edge.[14b] Since the theoretical electron scattering amplitude and phase were used in the later curve-fitting analysis, the normalized data (i.e. $[\mu(E) - \mu_0(E)]/\mu_0(E_0)$ with E_0 being the edge energy) were corrected by multiplying with a monotonic function $\mu_0(E_0)/\mu_0(E)$ obtained using the McMaster tables.[15] Figure 3 shows the magnitude of the Fourier transforms of the data.

The data analysis in this work was conducted using the nonlinear least-squares curve-fitting program EXAFIT written by Bauchspiess.[16] The parametrized function used to fit the data is the following

$$\chi(k) = \sum_j \frac{N_j}{k_j R_j^2} S_0^2 S(k_j) f_j(k_j) e^{-2k_j^2\sigma_j^2} e^{-2R_j/\lambda} \sin[2k_j R_j + \phi_j(k_j)] \quad (1)$$

where the sum is over all the neighboring atomic shells. N_j and R_j are respectively the mean internuclear distance between the central (absorbing) atom and atoms of the jth neighbor shell and the coordination number of the jth shell; $S_0^2 S(k)$ is a slowly-varying dimensionless function of k which describes the reduction of the EXAFS signal due to multiple excitation effects; σ_j^2 is the mean-squared relative displacement in R_j; λ is the mean free path of the photoelectron due to the finite core hole lifetime and interactions with the valence electrons; $|f_j(k_j)|$ is the magnitude of the backscattering amplitude of an atom in the jth shell; $\phi_j(k_j)$ is the scattering phase shift due to both the central and backscattering atom; and k_j is related to the experimental wavenumber of the photoelectron $k = [2m(E - E_{\text{inflection}})]^{1/2}/\hbar$ via the parameter ΔE_j (concerning the origin of the k_j scale) defined below

$$k_j = (k^2 - \Delta E_j/\gamma)^{1/2} \quad (2)$$

with $\gamma = \hbar^2/2m \approx 3.81$ eV Å^2. The effective backscattering amplitude $S_0^2 S(k_j)\ |f_j(k_j)| e^{-2k_j^2\sigma_j^2} e^{-2R_j/\lambda}$ and the phase $\phi_j(k_j)$ in (1) used in the fittings were calculated using an *ab initio* XAFS

(14) (a) See for example: Sayers, D. E.; Bunker, B. A. in *X-Ray Absorption: Principles, Application, Techniques of EXAFS, SEXAFS and XANES*; Koningsberger, D. C., Prins, R., Eds.; Wiley: New York, 1988; Chapter 6. (b) Two software packages have been used for the data reduction in this work: (i) EXAFS/APL Version 5, written by A. J. Seary, copyright 1984–1994; (ii) BAN Version 4.38, written by T. Tyliszczak, Tolmar Instruments, Hamilton, Ontario, Canada.

(15) McMaster, W. H.; Kerr Del Grande, N.; Mallet, J. H. *Compilation of X-ray Cross Sections*; National Technical Information Service: Springfield, 1969.

(16) Bauchspiess, K. R. Ph.D. Thesis, Simon Fraser University, 1990.

theory (FEFF)[17] in the single-scattering mode. S_0^2 has been shown to be insensitive to the chemical environment and can be approximated by the corresponding atomic value.[18] We assumed that the Zn, Cd, and Hg share approximately the same S_0^2 due to the same valence structure of the group 2B elements, and we used throughout the analysis $S_0^2 = 0.85$, which was calibrated for Cu.[17] The reasonableness of this choice can be seen from the correct coordination numbers yielded for the known structures of Zn_7-MT and Cd_7-MT. The curve-fitting was performed in both k-space on Fourier-filtered $k^3\chi(k)$ and in R-space on both the real and the imaginary part of the Fourier transform. The results were consistent with each other, and the average of the outcome in both ways was used as the final result. In the curve-fitting for the single shell, four parameters, namely ΔE, R, $\Delta\sigma^2$, and N, were varied simultaneously, where $\Delta\sigma^2$ is the difference between the resulting σ^2 value and the constant input in the FEFF calculation. The residual sum of squares used in this work is defined as[19]

$$\chi^2 = \frac{N_{pts}}{N_{pts} - n} \frac{1}{N} \sum_{j=1}^{N} (\text{Data}_j - \text{Model}_j)^2 \qquad (3)$$

where $N_{pts} = 1 + 2\Delta k \Delta R/\pi$ is the number of independent data points, n is the number of fitting parameters used, and N is the total number of data points. This is the quantity minimized in the nonlinear least-squares curve-fitting. For comparing the fits, the goodness-of-fit is defined as the χ^2_{min} normalized to the Fourier transform intensity. The uncertainties of the results were estimated by finding that deviation of a parameter from its best-fit value (by fixing this parameter while leaving all others floating) which doubles the residual sum of squares between the fit and data. This is illustrated in Figure 4 using the case for Hg_{18}-MT as an example. These uncertainties include all the effects of correlations between all the parameters, and the error bars estimated in the way described here could be too conservative.[19a] In the following we summarize the qualitative observations and quantitative analysis for the four metallothioneins studied in this work.

Zn_7-MT. Direct observation of the unfiltered $k^3\chi(k)$ data of Zn_7-MT (Figure 2) indicates that the EXAFS consists of only one set of modulated sinusoidal waves up to the high k end, i.e. only a single resolvable atomic shell is detected. This is more clearly demonstrated in the Fourier transform (see Figure 3); no significant peaks above the noise level beyond 2.5 Å are present. There is some residual intensity peaked around 3.8 Å in the Fourier transform which consistently exists under different transform windows (different k-space range and the order of k^n weighting) and has comparable intensity to the side lobes of the main peak. This intensity is too weak to be analyzed reliably, however. These observations are different from the result reported previously by Abrahams et al.,[8b] where several distinguishable bumps in the high R region were interpreted as higher shells of S and Zn. The sample preparation procedures and the EXAFS experimental conditions in this work are similar with those reported in ref 8b. In view of the better data quality in this work, we believe that the bumps in the high R region of the Fourier transform in ref 8b were likely due to high-frequency noise in their data. The invisibility of any significant higher sheels indicates a rather large disorder in this system; however,

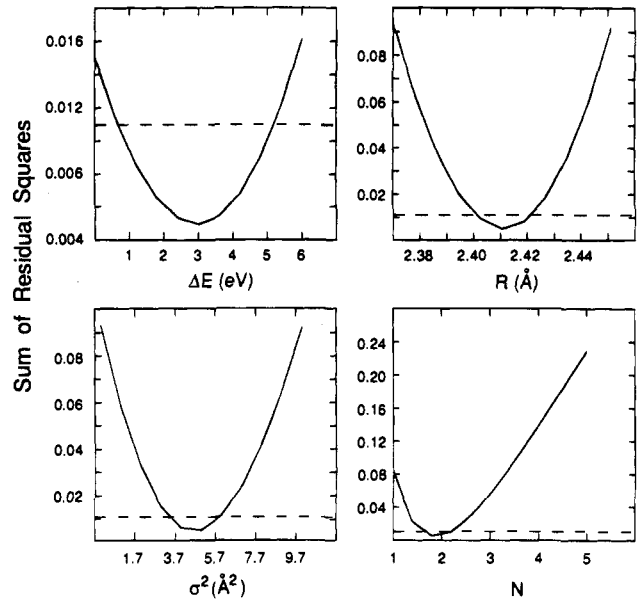

Figure 4. The exploration of the parameter space for the curve-fitting of Hg_{18}-MT 2. The sum of residual squares was obtained by fixing the individual parameter at the values shown on the x-axis while leaving the other three parameters floating to get the best fit. The horizontal dashed line intercepts the vertical axis where the sum of residual squares doubles its minimum value and the horizontal range between the two interceptions gives the error estimation for the parameter.

the short-range order (1st shell) is well-defined (see below). Whether the outer shells are detectable in EXAFS at even lower temperatures (e.g. at 10 K) is yet to be seen.

The peak around 2 Å in the Fourier transform is assigned to a single zinc thiolate coordination shell. The single shell assignment was checked with a beating analysis[20] which yielded a featureless phase-derivative vs k curve; this confirms that there are no different bond lengths (with comparable intensities) distinguishable under this shell. The Fourier transform (real and imaginary parts) of this shell and its Fourier-filtered single shell $k^3\chi(k)$ were curve-fitted in R- and k-space, respectively. The results are shown in Figure 5 (a and b) and Table 1.

The nearest neighbor bond length for Zn−S in Zn_7-MT was determined to be 2.349 ± 0.007 Å, and the thiolate coordination number was derived to be essentially 4, as expected for this well-known structure. The structural results in Table 1 for the first coordination shell of Zn_7-MT are in agreement with the values reported by Abrahams et al.,[8b] except the nearest neighbor bond length is slightly longer, by about 0.02 Å. The significance

(17) (a) Rehr, J. J.; Mustre de Leon, J.; Zabinsky, S. I.; Albers, R. C. *J. Am. Chem. Soc.* **1991**, *113*, 5135−5140. (b) Mustre de Leon, J.; Rehr, J. J.; Zabinsky, S. I.; Albers, R. C. *Phys. Rev. B* **1991**, *44*, 4146−4156.

(18) Stern, E. A. in *X-Ray Absorption: Principles, Application, Techniques of EXAFS, and XANES*; Koningsberger, D. C., Prins, R., Eds.; Wiley: New York, 1988; p 40.

(19) (a) Lytle, F. W.; Sayer, D. E.; Stern, E. A. *Physica B* **1988**, *158*, 701−722. (b) In the preceding reference the residual sum of squares suggested is

$$\chi^2 = \frac{N_{pts}}{N_{pts} - n} \frac{1}{N} \sum_{j=1}^{N} (\text{Data}_j - \text{Model}_j)^2/\delta_j^2$$

where δ_j^2 is the uncertainty of the jth data point which in principle includes a statistical part (due to random noise in each data point) and a nonstatistical part due to systematic errors. Usually the nonstatistical part is not known to each data point and the overall systematic error is estimated by fitting the known structures (e.g. the analysis of Zn_7-MT and Cd_7-MT data in this work provides an independent check on our analysis routine). When the data have a rather even distribution of random noise like the raw data shown in the Figure 2 (this is so because the data were taken with an uneven integration time at different k points), the weighting by δ_j^2 serves primarily as a scaling factor and has little effect on the estimation of the uncertainties. The dominant effect in the uncertainty is the correlation between the parameters, which has been included in the way of the uncertainty estimation in this work.

(20) See for example: Jiang, D. T.; Crozier, E. D.; Heinrich, B. *Phys. Rev. B* **1991**, *44*, 6401−6409 and references therein.

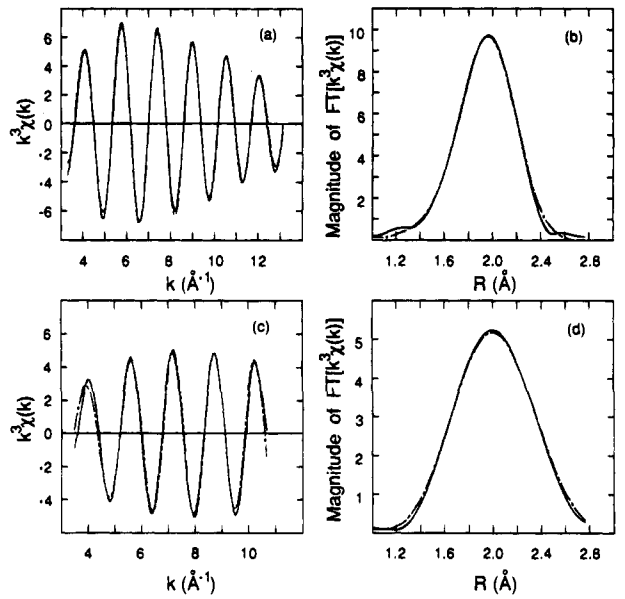

Figure 5. Left: $k^3\chi(k)$ of the Fourier filtered first shell data (solid) and the fit (dash). Right: The magnitude of the Fourier transform (solid) and the fit (dash) in R-space. Parts a and b are for Zn_7-MT 2, where the Fourier filtering window range is 1.04−2.72 Å. Parts c and d are for Cd_7-MT 2, where the filtering window range is 1.20−2.75 Å. The fitting ranges are as shown in the figure.

Table 1. Results of Nonlinear Least-Squares Curve-Fitting for the First Shell with S Scatters (Average of the Fits in R- and k-Space Shown in Figures 4 and 5)

	Zn_7-MT 2[a]	Cd_7-MT 2[b]	Hg_7-MT 2[c]	Hg_{18}-MT 2[d]
ΔE_0 (eV)	2.9 ± 2.1	0.8 ± 3.4	6.0 ± 3.5	3.0 ± 1.4
R (Å)	2.349 ± 0.007	2.50 ± 0.02	2.33 ± 0.02	2.41 ± 0.01
$\sigma^2 \times 10^{-3}$ (Å^2)	4.2 ± 0.8	2.8 ± 2.4	3.1 ± 1.9	4.6 ± 1.0
N	4.2 ± 0.5	4.2 ± 1.2	1.8 ± 0.5	1.9 ± 0.2
G[e]	0.0035	0.0068	0.0093	0.0020

[a] Previously reported Zn−S bond lengths, coordination numbers (CN), and XAFS Debye−Waller factor for Zn_7-MT at 77 K include R = 2.33(2) Å, CN = 4, and $\sigma^2 = 5 \times 10^{-3}$ Å^2 in rabbit liver MT.[8b,12] [b] Previously reported Cd−S bond lengths and CN for Cd_7-MT at 77 K include R = 2.53(2) Å, CN = 4, and $\sigma^2 = 6 \times 10^{-3}$ Å^2 in rat liver MT.[8a,c,12] [c] Previously reported Hg−S bond lengths and CN for Hg_7-MT at 77 K include R = 2.42(2) Å, CN = 3, and $\sigma^2 = 8 \times 10^{-3}$ Å^2. [d] See also Table 2. [e] The goodness-of-fit: χ^2_{min}/(R-space spectral intensity).

of analyzing data for a known structure mainly lies in establishing the validity of the analytical procedure that is to be used to tackle the novel systems discussed in the following.

Cd_7-MT. Figure 2b shows the k^3 weighted Cd K-edge EXAFS of Cd_7-MT, and Figure 3 shows the magnitude of its Fourier transform. The k-space range of the Cd_7-MT data set was shorter than that of the other sets because the photon energy was outside the optimum performance region of the Si(111) double crystals of the monochromator used in the experimental run. Again, a single coordination shell was assigned to the prominent peak around 2 Å in the Fourier transform spectrum. The bump between 4 and 5 Å does not survive consistently under various transform windows, so it is likely due to the large truncation artifacts in this particular case. The intensity and positions of other two peaks (between 3−4 and 5−6 Å, respectively) do persist under different testing transforms; therefore they may reflect the contribution of higher shell scatterers or some combination of various multiple scattering paths. The intensity of these two peaks relative to the main peak increases as the order n of k^n weighting increases, which suggests they might be related to the heavier scatters in the system,[21] i.e. Cd in this case. A reliable interpretation of them is difficult considering the limited k-space data range and no attempt was made to quantitatively analyze these features in this work.

The data and fits for Cd_7-MT are shown in Figure 5, parts c and d, and the results of curve-fitting are again summarized in Table 1. The nearest neighbor bond length and coordination number are again in agreement with the previous literature values.[8a,c,12] The σ^2 (2.8×10^{-3} Å^2) obtained for Cd_7-MT appears much smaller than that in ref 8c (12×10^{-3} Å^2) and ref 12 (6×10^{-3} Å^2), respectively, although the measurements were all conducted at 77 K. The value obtained here is also smaller than that reported in ref 8a (6×10^{-3} Å^2 measured at 35 K). This is unlike the case of Zn_7-MT where the σ^2 (4.2×10^{-3} Å^2) is in much closer agreement with the value reported before (5×10^{-3} Å^2).[8b] The apparent large difference between σ^2 of Cd_7-MT in the cited references and the value obtained here is possibly due to the sometimes ambiguous definitions about the quantity (by a factor of 2) used in the early works rather than to a real difference in the data.

Hg_7-MT. Figure 2c shows the $k^3\chi(k)$ of Hg_7-MT. Without going into detail and by simply comparing the k-space EXAFS amplitude of Hg_7-MT with those of Zn_7-MT or Cd_7-MT (Figure 2) it can be seen that the thiolate coordination number in Hg_7-MT is about *half* of those in Zn_7-MT and Cd_7-MT, if contributions from the Debye−Waller factors and mean free path terms are assumed to be comparable in both cases. This means that the nearest neighbor (sulfur) coordination number is about 2 instead of 4. This result is striking in view of the widely believed model for Hg_7-MT that involves tetrahedral coordination; this result is also different from the only other previously reported result for Hg_7-MT, where the coordination number was concluded to be 3.[12] This observation will be elaborated upon in the following discussion when the results of the curve-fitting analysis are described and the significance will be discussed in the Discussion section. In the Fourier transform of Hg_7-MT (shown in Figure 3) there are more features beyond the main peak around 2 Å in contrast to that of Zn_7-MT which has a similar k-space data range. The peaks at about 2.8 and 4 Å are real features judging by their stability under transform using different windows (different k range and k^n weighting). The relative intensities of these peaks are rather insensitive to different order of k^n weighting, so they may be due to a contribution of atoms of both the heavy and light elements;[21] i.e. Hg and S in the current case, from a similar distance. The features in the Fourier transform below 1.5 Å are partially due to residual background in the k-space data, since they are well-separated from the main peak so the analysis is not affected by them.

The single shell curve-fittings of the main peak in the Fourier transform are shown in parts a and b in Figure 6 in k- and R-space, respectively, and the results are summarized in Table 1. The nearest neighbor bond length thus obtained is 2.33 ± 0.02 Å, with a coordination number of ~2. Fits with the coordination number fixed at 3 and 4 were tested and rejected: the resultant sums of residual squares were more than 5 times larger than the results shown in Table 1, and there are no minima found around these N values when the parameter space was explored along this parameter from 0 to 5. The nearest neighbor bond length obtained here is much shorter than the one reported before as 2.42 ± 0.02 Å in ref 12. (The Hg−S value reported previously[12] at 2.42 ± 0.02 Å is surprisingly close to our value of 2.41 ± 0.01 Å for Hg_{18}-MT to be discussed below.) No

(21) Woolery, G. L.; Powers, L.; Winkler, M.; Solomon, E. I.; Spiro, T. G. *J. Am. Chem. Soc.* **1984**, *106*, 86−92.

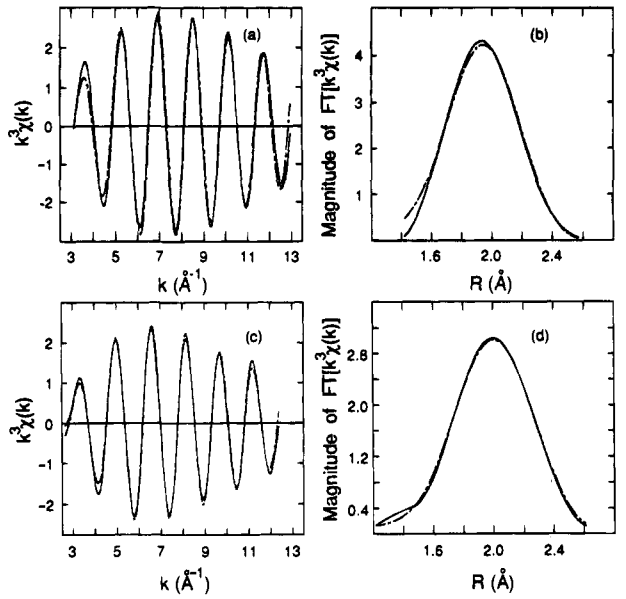

Figure 6. Left: $k^3\chi(k)$ of the Fourier filtered first shell data (solid) and the fit (dash). Right: The magnitude of the Fourier transform (solid) and the fit (dash) in R-space. Parts a and b are for Hg_7-MT 2, where the Fourier filtering window range is 1.42–2.57 Å. Parts c and d are for Hg_{18}-MT 2, where the filtering window range is 1.20–2.62 Å. The fitting ranges are as shown in the figure.

acceptable results were observed for fitting the main peak with two different Hg–S shells or a mix of Hg–S and Hg–Cl shells; the results for the second Hg–S or Hg–Cl shell have a negligible coordination number (<0.05) and a negative σ^2.

The curve-fitting cannot actually distinguish between nearest neighbors of the elements S and Cl, but a test of fitting with O as the nearest neighbor clearly yielded nonphysical results, e.g. negative coordination numbers.

Fitting was also attempted on the feature around 2.8 Å in the Fourier transform using single scattering paths with a shell of two S. When the ratio of coordination number for this feature over that of the main shell was fixed at 1 (i.e. assuming this feature also represents a shell with coordination number 2), the bond length obtained was between 3.33 and 3.45 Å (depending on whether ΔE_2 was varying relative to that of the first shell), but the resulting σ^2 was about 20×10^{-3} Å^2, which is too large for the EXAFS expression in (1) to be reliable. This indicates that if the 2.8 Å feature in the Fourier transform originated from a remote S shell, this shell would have a large and non-Gaussian disorder which goes beyond the domain of validity of the small disorder approximation which equation 1 is based on. The estimated bond length of the distant coordination shell is approaching the sum of the van der Waals radii of Hg and S[22], therefore the secondary interaction between the Hg and S in the cluster is very weak, which may explain the large σ^2 obtained above.

Hg_{18}-MT. Figures 2d and 3 show the EXAFS and the Fourier transform for Hg_{18}-MT. Just as for Hg_7-MT, it can be seen that the Hg_{18}-MT EXAFS amplitude is about half that of both Zn_7-MT and Cd_7-MT, where the coordination number is 4. The Fourier transform also shows a dominant peak around 2 Å and some small bumps in the higher R region which are real features confirmed by the same procedure as in the other cases described above. However, the intensity is too weak to be quantitatively analyzed. Again, the intensity below 1 Å is partially due to the residual background in the k-space data.

(22) (a) Canty, A. J.; Deacon, G. B. *Inorg. Chim. Acta* **1980**, *45*, L225–227. (b) Bondi, A. *J. Phys. Chem.* **1964**, *68*, 441–451.

Table 2. Results of Nonlinear Least-Squares Curve-Fitting for Hg_{18}-MT 2 (Two-Shell Model, Average of the Fits in R- and k-Space)[c]

	ΔE_0 (eV)	R (Å)	$10^{-3}\sigma^2$ (Å^2)	N
Hg–S	5.9 ± 5.0	2.42 ± 0.026	4.3 ± 4.2	2.0 ± 0.8
Hg–Cl	5.9[a]	2.57 ± 0.03[b]	11.6	0.61

[a] The difference between this value and that of Hg–S was fixed at zero in fitting. [b] Estimated from the difference between the fits in k- and R-space. [c] Goodness-of-fit: χ^2_{min}/(R-space spectral intensity) = 0.0020.

The similarity between the transforms of Hg_{18}-MT and Hg_7-MT should be noted (see Figure 3).

Fits for the main peak in the Fourier transform of the Hg_{18}-MT data are shown in Figure 6, parts c and d, and the results of the fits are summarized in Table 1. The bond length and coordination number are 2.41 ± 0.01 Å and (essentially) 2, respectively. Testing fits with the coordination number fixed at 3 yielded results with ~10 times larger sum of residual squares. Exploration in the parameter space along N showed no other minima except the one near 2 (see Figure 4d). The data only allow the coordination number to be 2 for a model of a single element shell. However, in contrast to the Hg_7-MT case, a model in which Hg–S bonds coexist with Hg–Cl bonds under the main peak in the Fourier transform also seems acceptable. The two-shell fitting results are listed in Table 2. In this fitting the difference in ΔE_0 between the two shells was fixed at zero to limit the correlation between the parameters. The two-shell fitting has similar sums of residual squares as that for the single Hg–S shell model but the uncertainties of the parameters are significantly increased due to the remaining correlation between the parameters. In this two-shell model, besides the 2 Hg–S bonds which are practically the same as in the single shell fit, there is a Cl shell at 2.57 Å with an apparent coordination number of 0.61 and a large σ^2 (11.6×10^{-3} Å^2). The large σ^2 indicates that the Cl shell has a large disorder and could involve more complicated structures than the single bond length structure assumed in the model. Considering the limited spectral features, no more detailed modeling was attempted for the Hg–Cl shell. Because the Hg–Cl shell constitutes a small fraction of the main peak in the transform, the method of error bar estimation carried out for the dominant Hg–S shell is not practical for the error estimation of the parameters of the Hg–Cl shell. Therefore, no error bars were assigned to the coordination number and σ^2 of the Hg–Cl shell and these two strongly correlated parameters should be viewed as a collective pair to represent the intensity of the Hg–Cl shell. The error bar of the bond length of the shell was estimated from the deviations of different fits conducted in k- and R-space (Table 2). Since S and Cl are indistinguishable as backscattering neighbors, two different Hg–S shells also yielded similar results. This latter model is considered less favored because of the known Hg–S stoichiometry in the sample and the crucial dependence of the formation of Hg_{18}-MT on the existence of chloride ions (see in the Discussion section). In k-space there is a partial cancelling effect between the components of Hg–S at 2.42 Å and Hg–Cl at 2.57 Å, which accounts for why the main peak in the transform could accommodate a weak Hg–Cl shell and at the same time exhibit a slightly increased intensity (i.e. smaller σ^2 and larger N) for the Hg–S shells compared to the single shell fitting discussed above.

Figure 7 shows the X-ray absorption near edge structure (XANES) and its derivative for Hg_7-MT and Hg_{18}-MT. Clearly the local structures reflected by these spectra are similar to each other, the difference though is in the bond length which is clearly shown by the phase difference between the two sets of XAFS

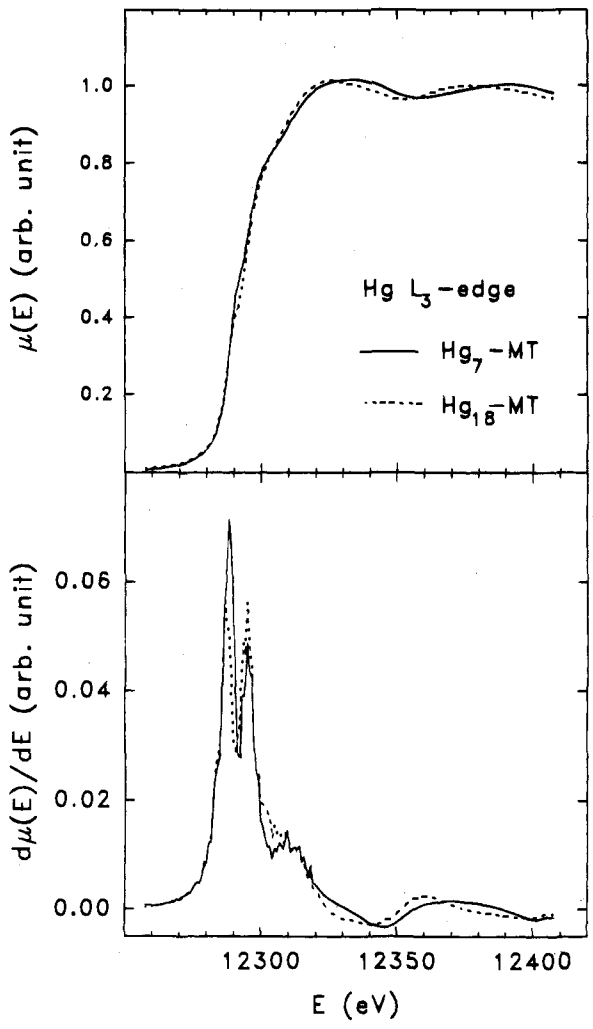

Figure 7. Comparison of Hg L_3-edge XANES for Hg_7-MT 2 and Hg_{18}-MT 2 (upper panel) and their derivatives (lower panel). The features below 12 320 eV are all similar and line up at the same photon energies. Above that energy it can be seen that the EXAFS oscillations of the two samples are out of phase due to different bond lengths.

wiggles. The similarity observed from the metal sites in Hg_7-MT and Hg_{18}-MT is in contrast to the difference between the two metallothioneins observed in the S $L_{2,3}$-edge XANES.[23] Comparison between the XANES taken at the Hg L_3-edge (from the point of view of metal atoms) and S $L_{2,3}$-edge[23] (from the point of view of S atoms) for the two samples may allow the S $L_{2,3}$-edge XANES spectra for Hg_7-MT and Hg_{18}-MT to be understood: the more complicated pattern observed in the S L-edge cases may simply arise from the presence of several kinds of binding sites for the S atoms in the system whereas there is essentially one type of site for Hg atoms.

It is interesting to note that the bond length for Hg_{18}-MT obtained here is virtually the same as that previously reported for Hg_7-MT (2.42 ± 0.02 Å) by Hasnain and co-workers.[12] These authors also concluded that the nearest neighbor coordination number and σ^2 of Hg_7-MT are 3 and 8×10^{-3} Å^2, respectively. Notice that our results on σ^2 for both Hg_7-MT and Hg_{18}-MT measured at 77 K (see Table 1) are all about half the magnitude of their values for Hg_7-MT (also measured at 77 K). A testing fit with σ^2 fixed at 8×10^{-3} Å^2 yielded a coordination number of 2.7, which then basically recovered the results of Hasnain *et al.* However, the result derived in such a way is likely to be in error because (i) the sum of the residual squares of the fit was 8 times larger than the best fit and (ii) the exploration in the parameter space did not show a minimum around this coordination value when σ^2 was also floating (Figure 4). The coordination number 3 for a single Hg−S shell obtained in ref 12 may have arisen by overlooking the correlation between N and the (over estimated) σ^2.

Before discussing the structural results, it is useful to examine the Debye−Waller factors in some detail to ensure that there is no significant underestimation of the mean-square relative displacement of the interatomic distance, σ^2. Generally σ^2 can be expressed as

$$\sigma^2 = \sigma^2_{vib} + \sigma^2_{stat} + \sigma^2_{dym} \tag{4}$$

where σ^2_{vib}, σ^2_{stat}, and σ^2_{dym} are the vibrational, static disorder (bonds with similar but not identical bond lengths), and dynamical disorder (ligand exchange) contributions, respectively.[24] The last term vanishes in solids at 77 K and the main contributions to σ^2 are then solely from the first two terms. The lowest limit of the vibrational term can be related to the totally symmetric vibration frequency of MS_4 and MS_2 moieties in the context of our discussion according to the following equation[25]

$$\sigma^2_{vib} = \frac{h}{8\pi^2\mu\nu}\coth\left(\frac{h\nu}{2kT}\right) \tag{5}$$

where μ is the reduced mass, ν the vibrational frequency, and k the Boltzman constant. The equation can be expressed numerically as

$$\sigma^2_{vib} = \frac{16.86}{\mu\bar{\nu}}\coth\left(0.72\frac{\bar{\nu}}{T}\right) \tag{6}$$

where μ is in grams/mole and $\bar{\nu}$ (the corresponding wavenumber) is in reciprocal centimeters. Typical M−S stretching wavenumbers are ~200−400 cm^{-1} for main group metals[26] and, in particular, for Zn−S, Cd−S, and Hg−S. Using $\bar{\nu}$ = 200 cm^{-1} the upper limit of σ^2_{vib} for a MS_4 cluster at 77 K is calculated as 2.7×10^{-3} Å^2, which is close but still smaller than the experimentally determined values of σ^2 (Table 1) as expected. The difference between σ and σ_{vib} can be partially attributed to static disorder, that is, the M−S bonds though similar are not necessarily identical. The R value obtained from EXAFS analysis reflects an average bond length of very similar bonds. This analysis further supports the validity of the curve-fitting results on σ^2.

Discussion

The remarkably diverse metal binding properties of the metallothioneins have attracted considerable attention.[1-11] Detailed studies of the binding of Zn(II), Cd(II), Cu(I), Ag(I), Au(I), Co(II), Fe(II), and Hg(II) have been reported.[1-5] The formation of metal thiolate cluster structures based on the stoichiometries M_4S_{11} and M_3S_9 (shown in Figure 8) for mammalian metallothioneins has been established by NMR for solution[1a,b] and X-ray diffraction for a crystal.[2] ^{1}H NMR studies[1c] show that the peptide wrapping in the Zn_7-MT and Cd_7-MT structures is essentially identical from the perspective of the peptide chain surrounding the metal binding site. In

(23) Lu, W.; Kasrai, M.; Bancroft, G. M.; Stillman, M. J.; Tan, K. H. *Inorg. Chem.* **1990**, *29*, 2561−2563.

(24) Sham, T. K.; Hasting, J. B.; Perlman, M. L. *J. Am. Chem. Soc.* **1980**, *102*, 5904−5906.

(25) Cyvin, S. J. *Molecular Vibrations and Mean Square Amplitudes*; Elsevier: Amsterdam, 1968; p 78.

(26) (a) Nakamoto, K. *Infrared and Raman Spectra of Inorganic and Coordination Compounds*; John Wiley & Sons: New York, 1978. (b) Baggio, R.; Frigerio, A.; Halac, E. B.; Vega, D.; Perec, M. *J. Chem. Soc., Dalton Trans.* **1992**, 1887−1892.

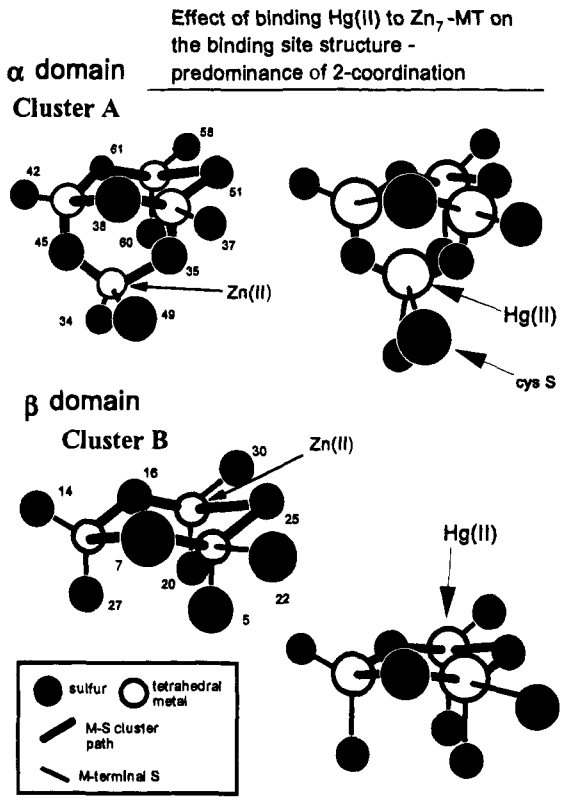

Figure 8. Left: The α and β domains showing the Zn−S clusters in rat liver Zn_7-MT 2 based on NMR[1] and X-ray[2] analysis. Right: The suggested model for Hg_7-MT 2 prepared by adding $Hg(NO_3)_2$ to Zn_7-MT 2 held at pH 7. For each Hg atom in this suggested model there are two short bonds (shown as heavy links) and two long bonds (light links) connected to the surrounding sulfur atoms. In the model, the mercury-containing clusters are flatter than those in the known structures of Zn_7-MT 2 or Cd_7-MT 2 shown on the left, and the S−Hg−S angle approaches 180°.

addition, S L-edge XANES[23] also suggest that the M−S environment for Cd_7-MT and Zn_7-MT is the same from the perspective of the coordinating sulfurs that are within the binding site.

Figure 8 represents the structure of Zn_7-MT and shows how each zinc is tetrahedrally coordinated by a combination of bridging and terminal cysteinyl thiolate groups. While previous spectroscopic data established that the cluster structure shown in Figure 8 exists for mammalian Cd_7-MT and Zn_7-MT,[1-4] the question remains as to the structures involving other metals (especially Hg(II)). Only a few metals are spectroscopically active (^{113}Cd and ^{119}Hg by NMR, Co(II) by EPR), and proton NMR experiments are unable to determine the metal−thiolate connectivities other than by inference. Clearly then, the metal−thiolate (M:S) stoichiometric ratio provides the most sensitive clue to possible structural patterns. M:S values have been determined and verified for a number of metals.[3e] For Hg-MT, we have described CD spectral data that clearly indicate metal-to-protein ratios of 7, 11, and 18 resulting in formation of well-defined structures.[10,11] We have used in this paper XAFS spectral data to study the structural properties of Hg(II), the third member of group 12, when it binds to mammalian metallothionein.

Spectroscopic studies some years ago established that Hg(II) displaced Zn(II) in Zn_7-MT to form Hg_7-MT,[5a] a complex with characteristic CD and magnetic CD (MCD) spectral properties. The saturation of the CD signal intensity at 7 Hg(II) suggested that mercury binding to metallothionein was the same as for Zn(II) and Cd(II). Efforts to determine structural information for Hg_7-MT using ^{199}Hg NMR were unfruitful due to the lability of the Hg(II) in the binding site.[5d] Detailed analysis of changes in the UV absorption spectrum as Hg(II) was added to Cd_7-MT at pH 7 suggested that a mixture of coordination geometries was present when between 5 and 9 Hg(II) were bound to Cd_7-MT.[5b] Analysis of CD spectral changes as Hg(II) was added to the metal free *apo*-MT, Zn_7-MT, and Cd_7-MT[11] provided the first evidence of a restrictive cage effect in which expansion of the binding site to accommodate the longer Hg−S bonds for tetrahedrally coordinated HgS_4 units is inhibited by the peptide linkages between the cysteinyl residues. These spectral data also identified a new class of metallothionein structure, Hg_{18}-MT.[10]

The data presented here clearly and unambiguously provide the necessary structural parameters that allow interpretation of the geometry adopted when mercury binds to mammalian zinc metallothionein. Structures of many mercury thiolate complexes have been reported: 2.32 Å is typical for linear coordination, 2.44 Å is typical for trigonal coordination and 2.52 Å is typical for tetrahedral coordination.[27] Mercury frequently forms two short bonds to sulfur and two longer bonds to other sulfurs or halides.[28]

In the following we first give a brief account of our results with Zn_7-MT and Cd_7-MT and then focus the discussion on the mercury-containing metallothioneins.

Zn_7-MT 2 and Cd_7-MT 2. The coordination number (CN) of both cadmium and zinc is, as previously reported,[8a,c,12] derived to be CN = 4 (Table 1). The bond lengths of 2.50 (Cd) and 2.35 (Zn) Å are in close agreement with previously reported values.[8a,c12] For Zn_7-MT the difference between our results and those previously reported is that there is no indication in our data that remote S and Zn scatters can be detected. In view of the better data quality in this work we believe that the remote S and Zn shells reported in ref 8b are not reliable.

Hg_7-MT. The Hg EXAFS data for both Hg_7-MT 1 and Hg_7-MT 2 formed from Zn_7-MT at pH 7 are essentially the same and significantly different when compared with the EXAFS data for Cd_7-MT 2 and Zn_7-MT 2. The results from the analysis directly allow interpretation of the CD data previously reported.[11] For the purposes of this discussion we consider the coordination around a single Hg(II). The first shell with CN = 2 has a bond length of 2.33 Å, and a possible second shell bond length is less well defined at 3.4 Å. These bond lengths clearly do not identify a tetrahedrally coordinated HgS_4 structure which should have average bond lengths of about 2.52 Å.[27] However, the two short bonds of 2.349 Å and the two long bonds of 3.234 Å (with an angle at the Hg between the long bonds of 71.7°) in $[Hg(SC_6H_4\text{-}2\text{-}SiMe_3)_2]$[29a] suggest an explanation. In Hg_7-MT formed from Zn_7-MT at pH 7, the binding site cage is too small to accommodate the volume of tetrahedral HgS_4 units. The peptide chain that connects each cysteinyl thiolate introduces a restriction not found with inorganic thiolates by locking the spacial distribution of the cysteines into a distribution initially set when the Zn(II) was bound. Simply, the mercury thiolate cluster structure that forms as Hg(II) displaces Zn(II) can only occupy a certain volume within the "Zn" binding site before the connecting peptide is stretched too tight, forcing some form of rearrangement. Metal binding to metallothionein is dependent on temperature, with considerable

(27) Gruff, E. S.; Koch, S. A. *J. Am. Chem. Soc.* **1990**, *112*, 1245−1247.
(28) Govindaswamy, N.; Moy, J.; Millar, M.; Koch, S. A. *Inorg. Chem.* **1992**, *31*, 5343−5344.
(29) (a) Bloch, E.; Brito, M.; Gernon, M.; Mcgowty, D.; Kang, H.; Zubieta, J. *Inorg. Chem.* **1990**, *29*, 3172−3181. (b) Alsina, T.; Cless, W.; Fraser, K. A.; Sola, J. *J. Chem. Soc., Chem. Commun.* **1992**, 1010−1011.

inhibition of cluster formation being observed below 15 °C.[4b] Hence the overall shape of the metal binding site cage can also be fixed by the displaced Zn(II). The interconnected lattice in the M_4S_{11} and M_3S_9 clusters does not readily allow for the thiolates to be moved, unless the tetrahedral orientation around the incoming metal is lost.

We propose that as Hg(II) is added to Zn_7-MT the binding site cage distorts but the interconnected bridging and terminal thiolates restrict the possible local geometries for the HgS_4 units. (Based on the known chemistry of Hg(II) in the presence of thiolates[28] and on the reported subsequent reaction to the Hg_{11}-MT complex,[11] we have to assign each of the 20 cysteinyl thiolates to some form of Hg−S bonding.) This rearrangement leaves a distorted binding site cage with each Hg(II) digonally coordinated to two thiolates with unusually short Hg−S bonds (2.33 Å) and to two thiolates with unusually long bonds. Other Hg-containing compounds also exhibits this 2 short, 2 long phenomena.[29] Recently, Koch and co-workers[28] have described just this situation for inorganic compounds.

The intensity in the EXAFS Fourier transform associated with a bond length of ~3.4 Å could be a manifestation of the longer bonds in the distorted tetrahedral cluster. Further addition of Hg(II) at pH 7 results in the collapse of this structure because the Hg(II) can bind trigonally[27] and linearly,[27,28] so that subsequent structures continue to form at greater metal-to-protein stoichiometric ratios.

We must emphasize that the controlling feature for the structure of the binding site in Hg_7-MT is that there is a deficiency of Hg(II) to bind the available thiolates without adopting a geometry with a coordination number of 4; but the steric restrictions imposed by the structure of the coordinating cysteinyl thiolates result in the observed distortion from CN = 4. Thus, Cu(I) and Ag(I) appear to form structures based on trigonal coordination but 12 metals are required.

Hg_{18}-MT 2. Addition of 18 Hg(II) to the Zn_7-MT 2 complex held at pH 2 is characterized by a unique CD spectrum.[10] Chemically, formation of the Hg_{18}-MT discriminates between isoform 1 and 2 of rabbit liver metallothionein.[10] Rat liver metallothionein binds 18 Hg(II), but the complex formed does not exhibit the CD spectrum observed for the rabbit liver protein.[10] These observations have been used previously to propose that the Hg_{18}-S_{20} complex forms as a single domain involving digonal S−Hg−S coordination with possibly distant chloride coordination necessary to account for the strong chloride ion dependence.[10b]

As shown in Tables 1 and 2, the Hg−S bond lengths of Hg_7-MT (2.33 Å) and Hg_{18}-MT (2.41 Å) are distinctly different, indicating different structures around the metal-binding sites. This unambiguously shows that the characteristic CD spectrum of Hg_{18}-MT[10] indeed represents a new kind of metal thiolate cluster. From the single shell fit, the sulfur coordination number associated with the 2.41 Å bond length is determined to be ~2 (Table 1). However, the value for the Hg−S bond length in Hg_{18}-MT does not match the typical bond length for CN = 2 inorganic thiolates, as the latter should be about 2.32 Å.[27] In fact, the 2.41 Å bond length determined for Hg_{18}-MT is very close to the well-accepted Hg−S bond length for trigonal coordination (2.44 Å[27]) in inorganic mercury thiolate complexes. The two-shell fit discussed previously does seem to suggest that a distorted trigonal local geometry is present in Hg_{18}-MT. While it is initially difficult to judge which of the two fits is more reasonable from the EXAFS analysis alone, we can examine the validity of the two-shell model by considering the rather strict conditions for the formation of Hg_{18}-MT 2 and the corresponding structural consequences. The formation of Hg_{18}-MT requires the presence of an *excess amount* of chloride ions.[10b] CD spectroscopy has indicated that only in the presence of high concentrations of Cl^- (equal or above 300 mol equiv) does a well-defined Hg_{18}-MT 2 structure form.[10b] The known structure of a Hg^{2+}−L-cysteine complex, $HgCl_2[SCH_2CH(NH_3)COOH]$, may provide some hints about the effect of chloride ion(s) on the Hg−S bond length. In this compound, the mercury atom is coordinated by two sulfurs at 2.453 and 2.490 Å, respectively, and two chloride ions at 2.582 and 2.645 Å, in a distorted tetrahedral geometry.[30] Here the first nearest neighbor shell (Hg−S) adopts an average bond length shorter than the characteristic value of 2.52−2.54 Å for a tetrahedral coordination under secondary interaction with the second nearest neighbor chloride shell. The situation in Hg_{18}-MT will be much more complicated due to the restrictions imposed by the peptide chain. Nevertheless, the above example of the inorganic compound shows that when chloride ions are present, the average Hg−S bond length is unusually short. Based on this model, we interpret the EXAFS data for Hg_{18}-MT using the two-shell fit in terms of 2 Hg−S bonds at 2.42 Å and a disordered Hg−Cl bond at 2.57 Å, overall a trigonal structure.

For the structure of Hg_{18}-MT, the question remaining is where the necessary chloride ion(s) are located relative to the Hg(II). Are they in the Hg−S cluster (e.g. under the main peak of the transform) or more distant? If the chloride ion(s) were located about 3 Å away (the only possible *distant* place where the EXAFS data indicated the existence of some scatters), it is difficult to understand the strong influence of the chloride ion(s), changing the Hg−S bond lengths from 2.33 Å that is characteristic of digonal coordination to the 2.42 Å of trigonal coordination. On the other hand, the model suggested by the two-shell fit accommodates the chloride ion(s) in the vicinity of the nearest neighbor sulfur shell with an indication of weak bonding between Hg(II) and the chloride ion(s). Therefore, although both of the fits for Hg_{18}-MT are acceptable from an EXAFS analysis point of view, the two-shell model is more satisfactory when taking into account the effect of chloride ion(s) on the formation of the Hg_{18}-MT structure. In summary, based on the EXAFS results presented here, the strong dependence of Hg_{18}-MT formation on the presence of chloride ions, and the easy deformability of the mercury thiolate bonding geometry illustrated in the inorganic compound discussed above, we conclude that the coordination of mercury in Hg_{18}-MT is with two sulfurs at the nearest neighbor distance (2.42 Å) and the necessary chloride ion(s) at a distance of 2.57 Å, in a distorted trigonal local geometry.

Conclusions

Structural parameters for Zn_7-MT, Cd_7-MT, Hg_7-MT, and Hg_{18}-MT have been obtained from analysis of metal EXAFS data obtained at 77 K. The derived nearest neighbor bond lengths of 2.349 ± 0.007 Å (Zn−S) and 2.50 ± 0.02 Å (Cd−S) are typical of tetrahedral coordination in the M_3S_9 and M_4S_{11} binding sites. These bond lengths are consistent with the coordination numbers of 4 for Zn_7-MT and 4 for Cd_7-MT. For Hg_7-MT the nearest neighbor Hg−S bond length is determined to be 2.33 ± 0.02 Å, the nearest neighbor coordination number to be 2, and the σ^2 to be (3.1 ± 1.9) × 10^{-3} Å^2. A new structure consistent with our data is proposed for Hg_7-MT formed from Zn_7-MT at pH 7 in which each Hg(II) is coordinated by four thiolates but with two unusually short bonds (2.33 ± 0.02 Å) and two unusually long bonds (possibly ~3.4 Å) which have a much larger disorder than the shorter bonds. The structure of

(30) Taylor, N. J.; Carty, A. H. *J. Am. Chem. Soc.* **1977**, *99*, 6143−6145.

the Hg_{18}-MT species is shown to involve Hg−S bond lengths of 2.42 ± 0.026 Å with the coordination number to be 2 and σ^2 to be (4.3 ± 4.2) × 10^{-3} Å^2, plus a Hg−Cl shell with a bond length of 2.57 ± 0.03 Å and apparent coordination number and σ^2 of 0.61 and 11.6 × 10^{-3} Å^2, respectively. The analysis confirms that the Hg(II) coordinates to two thiolates which, when the Hg_{18}-S_{20} stoichiometry is considered, requires a structure involving bridging thiolates in a single, clustered domain.

Acknowledgment. We thank Dr. W. Lu for preparing the samples used in this study. D.T.J. thanks Prof. E. D. Crozier for providing the computing facilities used in data analysis of this work, Dr. X. R. Qin for help in the XAFS data acquisition, and the Natural Sciences and Engineering Research Council of Canada (NSERC) for a postdoctoral fellowship. The XAFS experiments were carried out at beamline X-11A at the National Synchrotron Light Source which is supported by the U.S. Department of Energy. This work was supported by grants from NSERC of Canada to T.K.S. and M.J.S. This is publication number 509 of the Photochemistry Unit at the U.W.O. T.K.S. and M.J.S. are members of the Centre for Chemical Physics at the U.W.O.